Control of growth and gut maturation by *HoxD* genes and the associated lncRNA *Haglr*

Jozsef Zakany[a], Fabrice Darbellay[b], Bénédicte Mascrez[a], Anamaria Necsulea[b,1], and Denis Duboule[a,b,2]

[a]Department of Genetics and Evolution, University of Geneva, 1211 Geneva 4, Switzerland; and [b]School of Life Sciences, Federal Institute of Technology, Lausanne (EPFL), 1015 Lausanne, Switzerland

Contributed by Denis Duboule, September 21, 2017 (sent for review July 13, 2017; reviewed by Nicoletta Bobola and Natasza Kurpios)

During embryonic development, *Hox* genes participate in the building of a functional digestive system in metazoans, and genetic conditions involving these genes lead to important, sometimes lethal, growth retardation. Recently, this phenotype was obtained after deletion of *Haglr*, the *Hoxd* antisense growth-associated long noncoding RNA (lncRNA) located between *Hoxd1* and *Hoxd3*. In this study, we have analyzed the function of *Hoxd* genes in delayed growth trajectories by looking at several nested targeted deficiencies of the mouse *HoxD* cluster. Mutant pups were severely stunted during the suckling period, but many recovered after weaning. After comparing seven distinct *HoxD* alleles, including CRISPR/Cas9 deletions involving *Haglr*, we identified *Hoxd3* as the critical component for the gut to maintain milk-digestive competence. This essential function could be abrogated by the dominant-negative effect of *HOXD10* as shown by a genetic rescue approach, thus further illustrating the importance of posterior prevalence in *Hox* gene function. A role for the lncRNA *Haglr* in the control of postnatal growth could not be corroborated.

lncRNA | digestive system | *Hox* regulation | growth control | CRISPR-cas9

Slow postnatal weight gain phenotypes can be induced by mutations in a range of genes important for developmental patterning. However, the molecular and physiological bases of such growth retardations are often difficult to pinpoint due to the high pleiotropy associated with these genes. While none of the 39 gene members of the *Hox* family has been included in this broad phenotypic class thus far, we noticed two cases of postnatal growth retardation during the several-years-long studies of our allelic series at the mouse *HoxD* locus. First, animals homozygous for a complete *HoxD* cluster deficiency showed about 30% body-mass deficit by the time of weaning. However, given that they suffered severe limb and innervation defects, growth retardation seemed compatible with reduced feeding (1). Secondly, a shorter deficiency removing *Hoxd1–Hoxd9* [$HoxD^{Del(1-9)}$] was associated with postnatal growth retardation in heterozygous mice in the absence of mobility defects. However, some specimens also displayed facial defects, again suggesting the existence of a physical problem potentially affecting the feeding behavior (2).

Highly severe postnatal growth retardation in the absence of any obvious malformations was recently reported following a targeted deletion of the *Hoxd* antisense growth-associated long noncoding RNA (lncRNA) *Haglr* in mice. This *midget* (*Mdgt*) phenotype, which was recorded in homozygous-mutant specimens (3), displayed a reduced viability attributed to a function of the lncRNA distinct from those associated with either *Hoxd1* (4, 5) or *Hoxd3* (6, 7), the two genes flanking *Haglr* in the *HoxD* cluster. Therefore, in these cases, both recessive and dominant phenotypes were recorded, and they were always associated with loci located in the anterior (telomeric) part of the *HoxD* gene cluster. In addition, other *HoxD* alleles showed midgut patterning defects, but their detailed analyses were made difficult by lethality at birth (8). Finally, distant *cis*-acting regulatory regions necessary for the transcriptional control of these genes in midgut were reported within the large regulatory landscape flanking this gene cluster on its telomeric side (9), emphasizing a potential link between growth retardation and alterations in gut development.

In this study, we tried to find a common explanatory framework for the various cases described above. We decided to complete the allelic series with a few more mutant chromosomes necessary to unambiguously interpret the previous observations relating phenotypes to particular genes. By using CRISPR/Cas9 mutagenesis in embryo, we demonstrate that the growth-retardation phenotype observed in $HoxD^{Del(1-9)}$ mice is caused by the dominant-negative effect of the HOXD10 protein. We also report comparable growth deficits in mice lacking the entire region from *Hoxd1* to *Hoxd4* [$HoxD^{Del(1-4)}$] (10) and that a mutation in the HOXD3 DNA-binding domain produces mice with similar growth deficits, in contrast to mice mutant for either HOXD1 or HOXD4. We document pathological signs of intestinal failure in three independent nested deletions. Together, these results converge toward a central role for *Hoxd3* in the growth-retardation phenotypes previously recorded and further explain the strong functional hierarchy at work among HOX proteins.

To address the potential function of *Haglr* in this context, we further engineered a pair of alleles carrying either a deficiency or an inversion of the CpG island containing the bidirectional promoter for both *Hoxd1* and the antisense lncRNA. Neither of these two alleles affected postnatal growth, even in the resulting absence of the reported *Haglr* RNA, suggesting that the *Haglr*-associated phenotype may result from an interference with *Hoxd3*

Significance

During development, transcription factors are necessary not only to pattern the body plan but also to control growth. However, the link between these two developmental components has been difficult to establish. *Hox* genes are involved in the emergence of a functional digestive system in metazoans, thus providing a potential impact on growth through nutrition. Also, genetic conditions involving these genes lead to important growth retardation. We analyzed several targeted mutant lines at the *HoxD* locus and found that stunted phenotypes can all be explained by the lack of function of *Hoxd3*, whose role seems to be critical in the developing gut of suckling mice, perhaps as an adaptation to the milk-dependent early postnatal period in mammals.

Author contributions: J.Z. and D.D. designed research; J.Z., F.D., and B.M. performed research; J.Z., F.D., B.M., A.N., and D.D. analyzed data; and J.Z. and D.D. wrote the paper.

Reviewers: N.B., University of Manchester; and N.K., Cornell University.

The authors declare no conflict of interest.

Data deposition: The data reported in this paper have been deposited in the Gene Expression Omnibus (GEO) database, https://www.ncbi.nlm.nih.gov/geo (accession no. GSE103086).

[1]Present address: Laboratory of Biometry and Evolutionary Biology, CNRS, University Claude Bernard Lyon 1, 69662 Villeurbanne, France.

[2]To whom correspondence should be addressed. Email: Denis.Duboule@epfl.ch.

This article contains supporting information online at www.pnas.org/lookup/suppl/doi:10.1073/pnas.1712511114/-/DCSupplemental.

transcription or mRNA stabilization rather than from a direct effect of the lncRNA as previously reported (11). As many of the severely stunted mutant mice largely recovered after weaning, we hypothesize that the suckling period and its particular physiological requirements may vitally depend on the function of the *Hoxd3* gene in the gut.

Results

Gain of Function-Dependent Growth Retardation. *Hoxd* deficiencies have been used extensively to study the complex regulation of this gene cluster (12). One of them involving the DNA interval from *Hoxd1* to *Hoxd9* [$HoxD^{Del(1–9)}$ or Del(1–9), discussed further below] (Fig. S1) resulted in a semilethal slow postnatal weight gain. Heterozygous males crossed with wild-type females produced the predicted 50% proportion of wild-type normal and 50% heterozygous offspring. Soon after birth, growth of half of the progeny lagged. Many growth-retarded individuals dropped below half their normal siblings' body mass and thus were killed following legal recommendation. However, the majority of growth-retarded specimens survived, and they were genotyped along with their killed littermates. All growth-retarded individuals carried a Del(1–9) chromosome (Fig. 1*A*; red labels), whereas all normally growing siblings were wild type (Fig. 1*A*; green labels). Wild-type individuals showed a peak of body growth between postnatal days (P)2 and P14, followed by a few days of slower growth. The growth curve then resumed and continued until the end of the seventh week.

After birth, however, growth of heterozygous Del(1–9) mutants was continuously retarded until the end of the fifth week. For survivors, growth did return, even though it remained depressed in some individuals as late as the end of the tenth week. The analysis of average body mass at 4 wk revealed that heterozygous Del(1–9) individuals had about half the body mass of their wild-type siblings. The comparison between a group of seven wild-type controls and 10 Del(1–9)-heterozygous siblings gave a statistically valid difference (Table 1). It is noteworthy that, once growth of mutant animals resumed, it reached slopes similar to those of their wild-type siblings weeks before. Therefore, while strong growth retardation occurred during milk feeding, growth could catch up after weaning in the surviving specimens.

Previously, we had observed in various alleles carrying partial deletions in the *HoxD* cluster (13) that the remaining gene located next to the breakpoint after the deletion had occurred was likely to adopt some of the expression specificities of the deleted genes. This observation, along with the dominant inheritance pattern of this Del(1–9) stock, strongly suggested a gain-of-function mechanism, because even a full deficiency of the *HoxD* cluster did not induce such severe growth retardation in heterozygous-mutant animals (1). Therefore, we suspected *Hoxd10* expression was gained in space and time and thus interfered with more anterior *Hox* gene function following the property of posterior prevalence.

Posterior prevalence was defined as the capacity of some posterior HOX proteins to override the function of more anterior ones when coexpressed in some contexts (14). As this property may rely upon the binding of these proteins on their DNA target sites, we induced a small deletion within the *Hoxd10* homeobox sequence *in cis* with the Del(1–9) deficiency by using the CRISPR/Cas9 technology in fertilized mouse zygotes. In this $HoxD^{Del(1–9)d10hd}$ allele, while the same Del(1–9) deficiency was present, the adjacent *Hoxd10* gene produced a protein that lacks its DNA-binding domain. The Del(1–9)d10hd founder animal had growth comparable to its wild-type littermates and was used to establish a stable mutant line.

Early postnatal growth of the Del(1–9)d10hd-heterozygous animals appeared normal, and females no longer showed atypical courtship, as previously reported for the Del(1–9) allele (2). Likewise, facial malformations were no longer recorded. Transheterozygous crosses generated wild-type, heterozygous, and homozygous offspring, as genotyped at 2 wk of age. By the end of the fourth week,

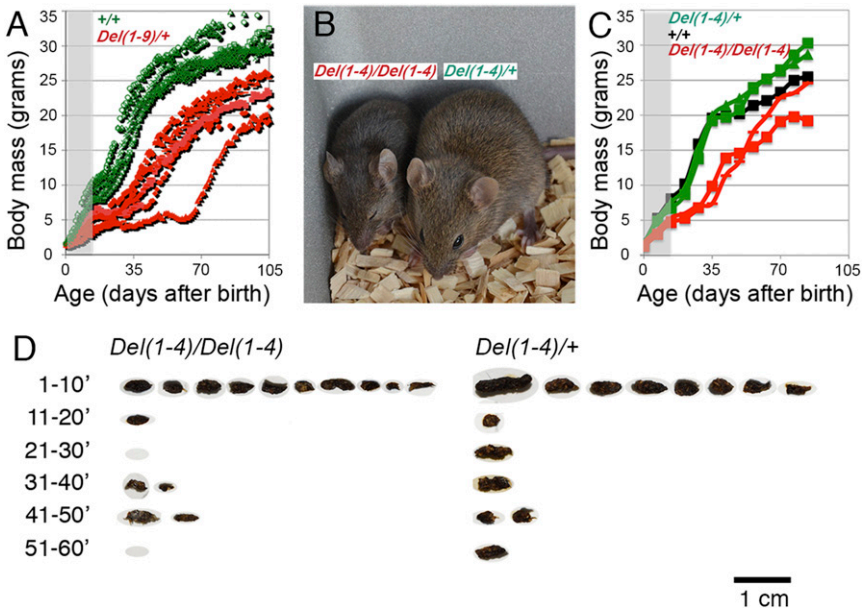

Fig. 1. Stunted growth, survival, and vital signs in mouse stocks carrying *HoxD* cluster deficiencies. (*A*) Growth trajectories of Del(1–9)-heterozygous (red) and sibling wild-type controls (green) expressed as a scatter diagram of individual daily body mass values. The gray zone on the left indicates that genotypes (determined at P14–P16) are still unknown at these time points, and colors are thus extrapolated from subsequent values. (*B*) A representative Del(1–4)-homozygous specimen (*Left*) and a heterozygous sibling on P21. (*C*) Growth trajectories of Del(1–4)-homozygous (red), -heterozygous (green), and wild-type control (black) siblings expressed as scatter diagrams of individual body mass values obtained on their day of birth and weekly thereafter. The gray zone is as in *A*. (*D*) Photographs of droppings released during six consecutive 10-min periods after isolation on P35 by a homozygous and a heterozygous Del(1–4) mutant. Individual dry pellet masses collected during daily 30-min periods of such defecation-reflex episodes were taken as ejected dropping mass, a noninvasive measure of gut function (*SI Materials and Methods*).

Table 1. Body weights of eight cohorts of various *HoxD* cluster mutants at age 4 wk

Genotypes	Average weight, g	SD	Fold change	Count	*P* value
+/+	14.5	1.71	1.00	7	
Del(1–9)/+	7.6	2.21	**0.52**	10	**4.55E-06**
+/+	12.8	1.29	1.00	5	
Del(1–9)d10hd/+	10.5	1.71	**0.82**	11	**1.33E-02**
Del(1–9)d10hd/Del(1–9)d10hd					
+/+	13.8	2.2	1.00	13	
Del(1–4)/+	12.5	2.55	0.91	28	2.17E-01
Del(1–4)/*Del*(1–4)	5.9	1.63	**0.43**	10	**9.09E-08**
+/+	11.3	1.82	1.00	3	
Del (4)/+	13.7	2.21	1.21	9	1.24E-01
Del (4)/*Del* (4)	12.4	2.92	1.10	3	5.98E-01
d3hd/+	11.0	1.96	1.00	3	
d3hd/Del(1–4)	7.4	0.57	**0.67**	4	**1.46E-02**
+/+	12.7	1.58	1.00	14	
d3hd/+	11.8	1.67	0.93	24	1.17E-01
d3hd/d3hd	8.3	2.15	**0.66**	20	**3.30E-07**
+/+	12.5	1.52	1.00	7	
Del(CpG114)/+	12.8	1.44	1.03	13	6.00E-01
Del(CpG114)/Del(CpG114)	11.8	0.87	0.95	8	3.04E-01
Del(1–4)/+	13.3	1.87	1.00	7	
InvCpG114/Del(1–4)	12.6	1.97	0.94	8	4.69E-01

Various *HoxD* cluster mutant genotypes and body weight statistics are grouped by crosses either between heterozygous and wild-type or between heterozygous animals. Statistical significance was calculated comparing mutants' body weight values with that of controls from the same cross. Four of fourteen heterozygous individuals in the *Del1–9*/+ class, all four homozygous individuals in the *Del(1–9)d10*^{hd}/*Del(1–9)d10*^{hd} class, and 8 of 23 homozygous individuals in the extended *Del*(1–4)/*Del*(1–4) class were killed during the second to fourth weeks due to severe stunting. Several of the *Del*(1–4)/*Del*(1–4) escaper individuals of both sexes bred successfully. In the extended *Hoxd3*^{hd} class, 2 of 24 homozygous individuals were killed during the second to fourth weeks after birth due to severe stunting. One escaper homozygous female bred successfully. *P* values in bold indicate a significant growth delay.

the mass of all homozygous animals dropped below the 40% limit in comparison with wild-type siblings, and hence animals were killed before the end of the experiment (Table 1). The comparisons of body mass averages between wild-type and heterozygous mice from two combined litters showed that the mass of heterozygous animals was only about 20% below the average mass of the wild-type controls. This was closer to normal than the nearly 50% deficit seen in presence of the intact *Hoxd10* locus *in cis* with the deficiency. This result demonstrated that a major factor in the dominant effects of the Del(1–9) allele was indeed due to a gain of function of *Hoxd10* after its relocation near the deletion breakpoint. The nearly 20% difference recorded between wild-type and Del(1–9)d10hd-heterozygous mice was statistically significant, suggesting that beyond the gain of function of *Hoxd10*, a combined loss of function of several genes *in cis* also had an impact upon the growth rate.

Loss of Function-Dependent Growth Retardation. Next we investigated a smaller deficiency including *Hoxd1* to *Hoxd4* [*HoxD*$^{Del(1–4)}$ or Del(1–4)], as homozygous specimens were severely retarded, and many did not survive to adulthood, thus further supporting a loss-of-function mechanism being causative of growth retardation. This was unexpected, since previous targeted loss of function of *Hoxd1* (4, 5), *Hoxd3* (6, 7), or *Hoxd4* (15) did not reveal such growth retardation. This phenotype was highly reproducible and was stable over generations, and homozygous escapers were visibly smaller than normal (Fig. 1*B*). The growth curves of homozygous, heterozygous, and wild-type controls from the same litter and fed by the same dam showed that homozygous specimens lagged in much the same way as Del(1–9)-heterozygous escapers (Fig. 1*C*). In both conditions, the retardation was similarly recorded by the end of the first week, and animals continued to grow at a reduced rate compared with heterozygous or wild-type littermates until the end of the seventh week. One homozygous animal continued to grow at a relatively steady rate until it caught up with the wild type by the end of the 11th week, whereas the other reached about 80% of wild-type body weight.

Several such caught-up individuals otherwise proved healthy and fertile. However, more than half of them dropped below 40% of control sibling body mass before the end of the seventh week. Growth trajectories diverged during the period of milk feeding. From these results, a genetically determined period of sensitivity seems to occur between birth and the end of the fourth week. This period was characterized by a reduced capacity to thrive despite the ability to feed. While wild-type and heterozygous body mass values were not appreciably different (Table 1), the average body mass of homozygous individuals was well below half the average of the wild-type individuals. This was comparable to the body mass deficit we observed with Del(1–9)-heterozygous mice, and the recovery of the homozygous Del(1–4) individuals was also similarly shifted (Fig. 1, compare *A* and *C*). We also observed that Del(1–9)d10hd-heterozygous displayed twice as great a body mass deficit as Del(1–4)-heterozygous (*Discussion*).

Coprometric Investigation of Slow Postnatal Weight Gain. In our daily observations of litters including either Del(1–9)-heterozygous or Del(1–4)-homozygous individuals, we noticed that growth-retarded animals were weak and lethargic. In addition, they dropped few or no fecal pellets. We used the latter observation as a noninvasive measure to characterize and follow the phase of recovery. Analysis of droppings reveals species-specific features of excretory activity (16) and thus reflects the morphology and function of the intestinal tract. Such analysis can start after the end of the third week, once animals switch to solid food. In rodents, the gut content is liquid in the small intestine and paste-like in the cecum. The segmentation into pellets and dehydration occur along more distal colon segments.

When we collected the droppings in fractions, we found the majority was released in the first 10 min. Subsequently, their number dropped, indicating that this prolific early release was a defecation reflex (Fig. 1*D*).

In nearly all cases, the reflex gave comparable numbers of solid pellets per individual released by a similar dynamic. In addition, although the sizes of individual pellets varied, quite a few fell into in a rather narrow range. Finally, animals that suffered growth retardation produced smaller but not necessarily fewer pellets of similar consistency (Fig. 1*D*). The comparable solidity of up to 16 pellets per single collection suggested that sudden total pellet release represented the content of the terminal gut. On the other hand, the average or most frequent pellet sizes reflected a fairly regular size-setting mechanism that presumably operated at a more proximal segment. Because growth-retarded mutants released smaller pellets, we concluded that the gut was of a different anatomical and/or motile character compared with normal controls, while the mechanism of pellet segmentation and reflexive release were intact. As a consequence, we could evaluate gut performance individually in extended time series and in a reproducible noninvasive manner by measuring both the dried pellet mass collected in 30-min defecation-reflex periods and the body mass (Figs. 2–4 and Fig. S2).

***Hoxd3*-Dependent Growth Retardation.** Prior analysis of the combined deletion of *Hoxd1*, *Hoxd3*, and *Hoxd4* [Del(1–4)] revealed a drastic growth retardation in homozygous specimens (see above), which was not observed in either *Hoxd1* (4, 5) or *Hoxd4* (15) single-mutant mice. This could derive either from a combined effect of several gene products and the consequent compensatory mechanisms or from a prominent effect of *Hoxd3*. To discriminate between these possibilities, we produced a deficiency including the entire *Hoxd4* gene, $HoxD^{Del4}$ [Del (4)], as well as a *Hoxd3*-mutant allele. In the latter case, we used CRISPR-Cas9 to induce an out-of-frame deletion within the HOXD3 protein homeodomain, which presumably prevented HOXD3 from binding to DNA target sites.

Extensive analyzes of Del (4) mice revealed no significant growth defect in homozygous mice (Table 1). In contrast, F0 animals derived from the CRISPR/Cas9 mutation in *Hoxd3* (*SI Materials and Methods*) showed slow postnatal weight gain. Five apparently homozygous F0 animals indeed displayed this growth-retardation problem, even though this was not reported in previous evaluations of mutant *Hoxd3*-null alleles (6, 7). We crossed these F0 animals and analyzed progenies to confirm the link to *Hoxd3*. We first mated a $Hoxd3^{hd}$-mutant F0 female with a Del(1–4)-heterozygous male to obtain transheterozygous individuals and heterozygous controls, as well as to eliminate potential recessive off-target mutations since the Del(1–4) stock was generated without CRISPR/Cas9 exposure. However, Del(1–4)/+ animals were not recovered in the F1 progeny, showing that the F0 $Hoxd3^{hd}$ female was homozygous in the germ line. All $Hoxd3^{hd}$/Del(1–4) compound-mutant individuals were severely stunted (Table 1), and by P28, they reached only two-thirds of the body mass of their $Hoxd3^{hd}$/+-heterozygous siblings. This difference matched that observed between heterozygous and homozygous Del(1–4) specimens and was statistically significant (Figs. S1 and S2*C*).

Litters of F2 pups including all three possible $Hoxd3^{hd}$ genotypes were monitored, and wild-type and heterozygous females showed similar characteristics as we observed with F0 control males. However, their body weight at the end of the fast growth period at P42 was around 16 g, compared with the average of 20 g recorded with males (Fig. 2*A* and Fig. S2*A*). The body weight of wild-type and heterozygous individuals at the end of the third week was typically above 8 g Fig. 2*A*, *Left*), whereas most homozygous-mutant animals weighed less than 7 g (Fig. 2*A*, *Right*), and the most severely affected weighed less than 4 g (a more than 60% deficit compared with siblings of that age) (Fig. 2*A*). The body weight of the least-affected surviving homozygous individual ("escaper") rarely exceeded 12 g at the end of the seventh week (a deficit of *ca.* 25%) (Fig. 2*A*, *Upper*). To uncover a potential association with a gut defect, we recorded pellet masses from the beginning of the fourth week.

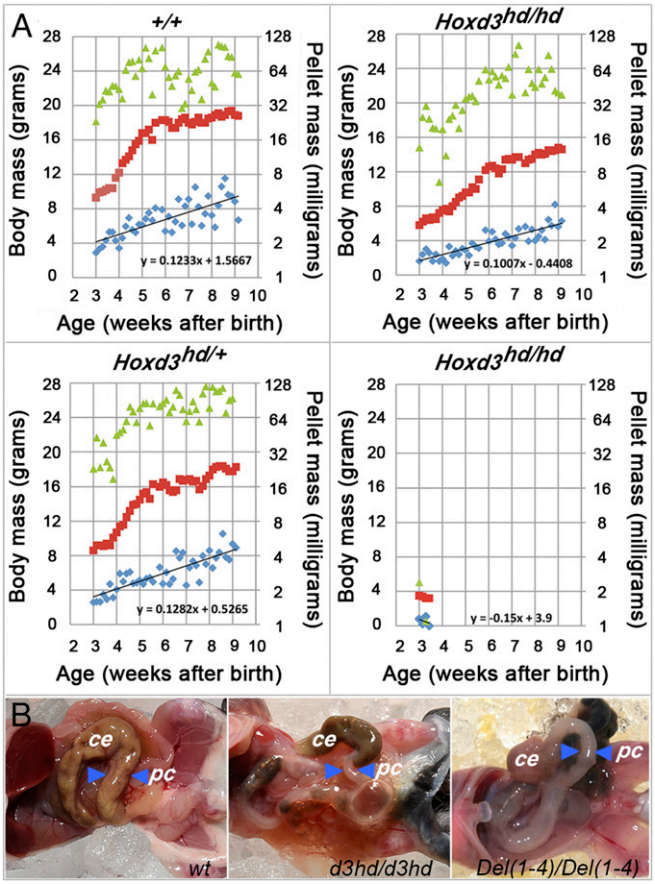

Fig. 2. Stunted growth, survival, vital signs, and gut malformation in $Hoxd3^{hd}$-homozygous mice. (*A*) Daily body mass (red), total dropping mass (green), and average dropping mass (blue) are plotted for wild-type (*Upper Left*) and heterozygous (*Lower Left*) mice and two homozygous siblings (*Right*). All four were females. The animal on the *Bottom Right* was killed at P23 due to severe stunting and wasting after weaning. Linear fitted lines show the dampened slope of average pellet mass for both homozygous animals. (*B*) Dissections of one representative individual of the three indicated genotypes showing the posterior midgut. Blue arrowheads point to the same segment of the proximal colon in each panel. The specimen on the *Middle* and on the *Right* were representative of severely wasted animals, usually killed during the fourth week after birth. ce, cecum; pc, proximal colon.

Like their wild-type siblings, heterozygous-mutant female mice regularly released more than 32 mg of total pellet weight on most days of the fourth week. During the fifth week and later, the total ejected weight was often in excess of 64 mg. In contrast, homozygous surviving females consistently released less than 32 mg of pellets during both the fourth and the fifth week and rarely reached 64 mg output by the end of the seventh week (Fig. 2*A*, *Upper*). Similarly, the average pellet weight of heterozygous and wild-type animals was about 4 mg by the end of the seventh week, while pellets of homozygous animals hardly ever reached this value even after the ninth week of age. It is noteworthy that most affected homozygous individuals released far fewer and smaller pellets and, during the terminal periods, released none at all (Fig. 2*A*, *Lower Right*).

Examination of the growth deficit including all F2 individuals at P28 also revealed a slight body mass deficit (7%) in the subpopulation of $Hoxd3^{hd}$-heterozygous individuals compared with

wild-type mice, even though this was of poor statistical significance (P value = 1.17^{-01}). In the homozygous subpopulation, however, the average body mass deficit was one-third of the average control body mass, a difference that was statistically significant. These observations supported the conclusion that *Hoxd3* is required for postnatal growth during the suckling period. Again, the distinctly reduced total ejected pellet mass during the fourth week suggested a decrease in the volume of the terminal segments of the gut. While the total ejected pellet mass slowly increased to reach nearly normal levels, the average size of pellets remained significantly smaller even at late stages (Fig. 3). This suggested a permanent loss of isometry in the initial formation of droppings and indicated that postnatal large bowel growth was likely delayed.

Morphological Alterations. The anatomical analysis of specimens from various genotypes revealed that droppings were already distinct in the more anterior part of the large bowel in the proximal colon. Consequently, we suspected that the proximal colon was morphologically or functionally insufficient in *Hoxd3*^{hd}-homozygous mutants. Also, in one particularly stunted mutant animal, while all abdominal organs were expectedly reduced in size (the total body mass was decreased by 60%), a clear retention of gut content in the terminal small intestine and in the cecum was recorded (Fig. 2*B*, *Right*). This distended region continued in a narrow empty proximal colon segment. Such a severe narrowing was also observed in Del(1–4)-homozygous stunted specimens (Fig. 2B, *Middle*). In agreement with the coprometric analyses, we concluded that this limitation in proximal colon diameter impeded the passage of luminal content and led to both reduced dropping size and reduced dropping deposition during an induced defecation reflex, leading over time to chronic constipation, malnutrition, and pronounced stunting.

Such a severe condition was further studied, in particular regarding the relative contribution of proximal and terminal colon defects to this slow postnatal weight gain. To this aim, we performed a correlation analysis of *Hoxd3*^{hd}-homozygous and wild-type control siblings. We plotted the body mass against average pellet mass, body mass against total ejected pellet mass, and the total ejected pellet mass against the average pellet mass. The R^2 values of wild-type controls were higher in the body mass versus average pellet mass comparison in all three phases than in the body mass versus total pellet mass comparisons (Fig. 4 *A* and *B*, blue). In the average pellet mass versus total pellet mass comparison, the R^2 value reached 0.56 during the growth period ($P <$ 1.17332^{-15}) but remained nonsignificant at later stages (Fig. 4*C*,

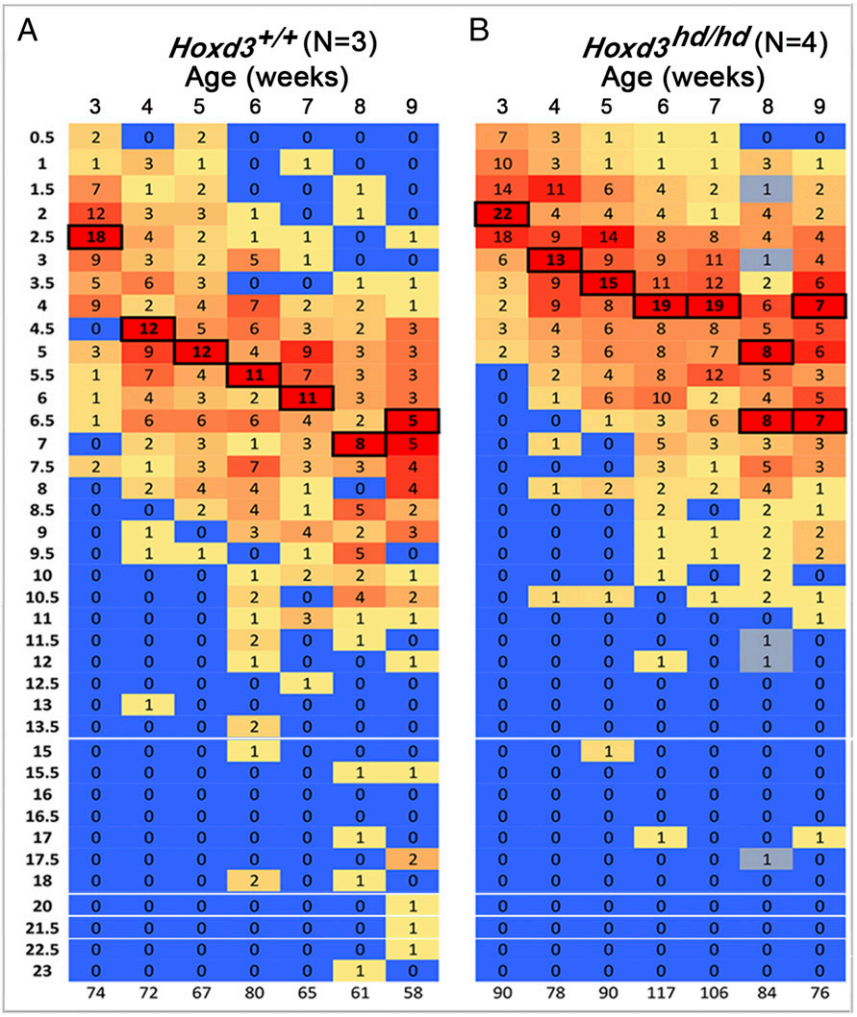

Fig. 3. Frequency distributions of dropping weights pooled from three wild-type controls (*A*) and four homozygous mutants (*B*). Age in weeks at the time of collection is indicated above, and the total counts of pellets collected during the last two consecutive days are shown below. The size bins set to 0.5-mg increments are indicated on the left. The heat maps reflect the relative frequency of pellet counts in a given lot; the most frequent values are boxed for better visibility.

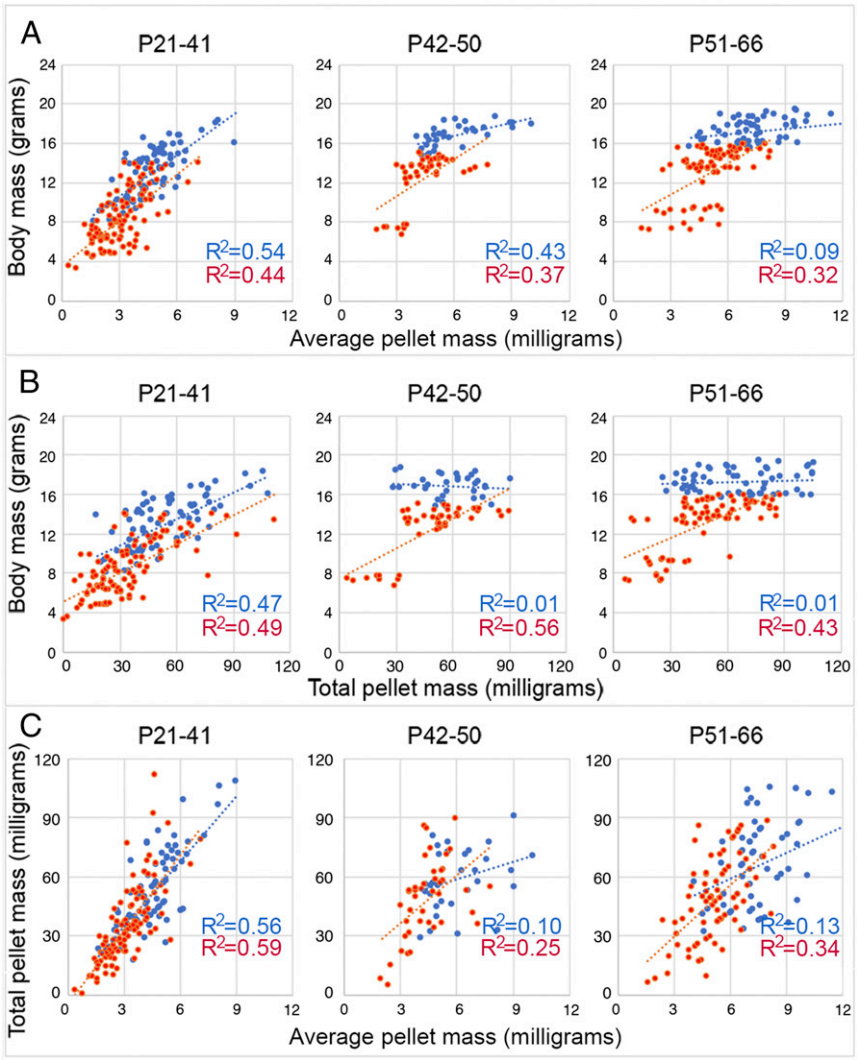

Fig. 4. Correlation analysis of body mass and dropping mass measures. Values from five wild-type controls (blue) and four homozygous *Hoxd3*^{hd} mutants (red) at three characteristic periods of wild-type controls' postnatal growth were pooled. Values were included from three different litters in which both controls and homozygous siblings occurred as members of the same litter. (*A*) Plots of body weight as a function of average pellet weight. (*B*) Plots of body weight as a function of total ejected pellet weight. (*C*) Plots of total ejected pellet weight as function of average pellet weight. Pellets released during single daily 30-min defecation-reflex episodes were included. In each plot, the R^2 values are depicted for wild-type (blue) and homozygous (red) animals to estimate the percentage of the variance due to variation in the respective parameter. R^2 values of 0.010 or below were not statistically significant; R^2 at 0.13 was statistically significant ($P < 0.005$); all other higher R^2 values were statistically significant ($P < 0.0005$ or far below).

blue). Average pellet mass was a better predictor of body mass than total ejected pellet mass.

Of note, the same comparisons applied to the *Hoxd3*^{hd}-homozygous samples diverged from this overall picture. The R^2 values were as high or indeed slightly higher in the body mass versus total pellet mass comparison than in the body mass versus average pellet mass comparison (Fig. 4 *A* and *B*, red). This was also confirmed in the average pellet mass versus total pellet mass analysis, and a positive correlation with delayed growth was established during all three periods. Average pellet mass and total pellet mass were positively correlated, and the correlation was of a higher degree at all stages compared with wild-type control (Fig. 4*C*, red). Average pellet mass as well as total ejected pellet mass were similarly good predictors of body mass in *Hoxd3*^{hd}-homozygous individuals. This correlation analysis therefore supported the inference that *Hoxd3*^{hd}-homozygous guts performed differently from those of wild-type control animals. Absolute values were nevertheless lower compared with controls, which was consistent with the idea that the reduced dimension of both proximal colon, as reflected in average pellet mass, and of the terminal colon, as reflected in total ejected pellet mass, contributed simultaneously to a strong constraint on organismal growth.

Epithelial Defects in *Hoxd3*^{hd}- and *HoxD*$^{Del(1–9)d10hd}$-Mutant Small Intestines. Following the abrogation of *Hoxd3* function, only about half of the variance in body mass could be accounted for by noninvasive coprometry. As body mass deficit first occurred before excrement could be collected, we investigated juvenile gut histology of stunted animals and normal littermates on P14 and P7. The duodenum of *Hoxd3*^{hd}-homozygous mutants and wild-type control siblings showed a reduction in diameter and in epithelium thickness (Fig. 5 *A* and *B*). When the body mass was plotted as a function of the average length of villi, it showed a positive correlation with the length of duodenum villi (Fig. 5*B*). Up to 90% of the variance in body mass could be accounted for by variation in duodenum epithelial structure.

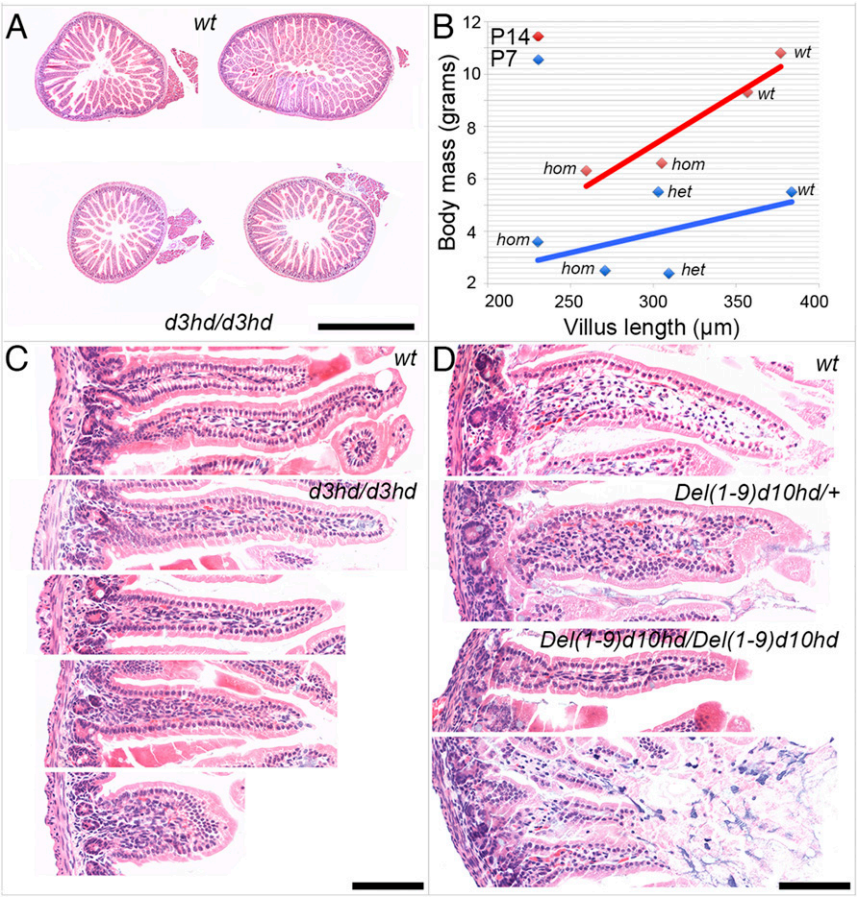

Fig. 5. Reduced small intestine diameter and epithelial dysgenesis in *Hoxd3*^{hd} and *HoxD*$^{Del(1–9)d10hd}$ milk-fed pups. (*A*) Two wild-type controls (*Upper*) and two *Hoxd3*^{hd}-homozygous siblings (*Lower*) are shown. (*B*) The longest villi from at least six available sections from each individual were selected and photographed, and their longest axis was measured. In the diagram the body weight was plotted as a function of the average longest villus length. The *Hoxd3*^{hd} stock at P14 is shown as red diamonds and a red line. The two diamonds on the right represent wild-type (wt) mice, and the two on the left represent homozygous (hom) siblings. A similar analysis was carried out with Del(1–9)d10hd at 7 d after birth and is depicted as blue diamonds and a blue line. The two values at the left represent homozygous animals (hom), the two in the middle represent heterozygous animals (het), and the one on the right is a wild-type control (wt). (*C*) H&E-stained paraffin sections of gut villi from wild-type control and two pairs of sections from two *Hoxd3*^{hd}-homozygous specimens showing representative morphologies. (*D*) High-power photomicrographs of H&E sections of wild-type and heterozygous specimens and from two Del(1–9)d10hd-homozygous animals showing representative morphologies. (Scale bar, 1 mm in *A* and 100 μm in *C* and *D*.)

Next we extended this analysis to Del(1–9)d10hd specimens and investigated wild-type control, heterozygous, and homozygous siblings 1 wk after birth. Examination of villus length also revealed a positive correlation between body mass and villus length (Fig. 5*B*). Body mass values were lower than at P14, consistent with the animals' younger age. Although a positive correlation was obtained between body mass and villus length, the slope of the fit line was clearly less steep than in the case of *Hoxd3*^{hd} mice at P14, and the R^2 value was only 0.28. Since body mass reduction and lethality was more severe in Del(1–9)d10hd animals, we surmised that changes beyond villus length contributed to the severity of this allele. More detailed observations using high-power images revealed reduced maximal villus length in both cases (Fig. 5 *C* and *D*). Del(1–9)d10hd-homozygous individuals also showed an extended region of villus disintegration (Fig. 5*D*, *Bottom*). The tips of villi were ill-formed, and more basal surfaces were devoid of the enterocyte layer, indicative of epithelial necrosis. From these histological observations, we concluded that early during milk feeding, epithelial dysgenesis occurred in *Hoxd3*^{hd}-homozygous mutants, which hindered proper alimentation of pups. This condition was further aggravated in the absence of an extended genomic locus, which in addition to *Hoxd3* removed *Hoxd10*, *Hoxd9*, *Hoxd8*, *Hoxd4*, and *Hoxd1* functions. These results further supported the hypothesis that gut defects were a cause rather than a consequence of small body size.

Contribution of the LncRNA *Haglr* to Growth Retardation. In a recent report, a similar semilethal recessive slow postnatal weight gain was observed upon disruption of the *Haglr* lncRNA, leading to the midget (*Mdgt*) phenotype (3). The *HoxD* antisense *Haglr* RNA starts from the *Hoxd1* bidirectional promoter and extends to the *Hoxd3* transcription unit. To further evaluate a potential function of this lncRNA on the growth-retardation phenotype, we produced two mutant alleles in which *Haglr* was presumably affected without removing the entire *Hoxd1–Hoxd3* intergenic region, which includes two other noncoding *Gm14426* and *Gm14424* RNAs (Fig. 6*A*). Transcriptome analysis of E8.5 embryos revealed that *Hoxd1* and *Haglr* share the same bidirectional start site located within the CpG island 114. On the reverse *Hox* strand, two *Haglr* start sites were mapped, as well as alternatively spliced transcripts including a short *Haglr* exon (Fig. 6*B*). We used CRISPR/Cas9 to produce two lines of mice, the first carrying a deletion of the CpG island 114 [*HoxD*$^{Del(CpG114)}$ or Del(CpG114)] and the second carrying an inversion of the same DNA fragment [*HoxD*$^{Inv(CpG114)}$ or Inv(CpG114)]. Nine Del(CpG114) F0 founders were obtained

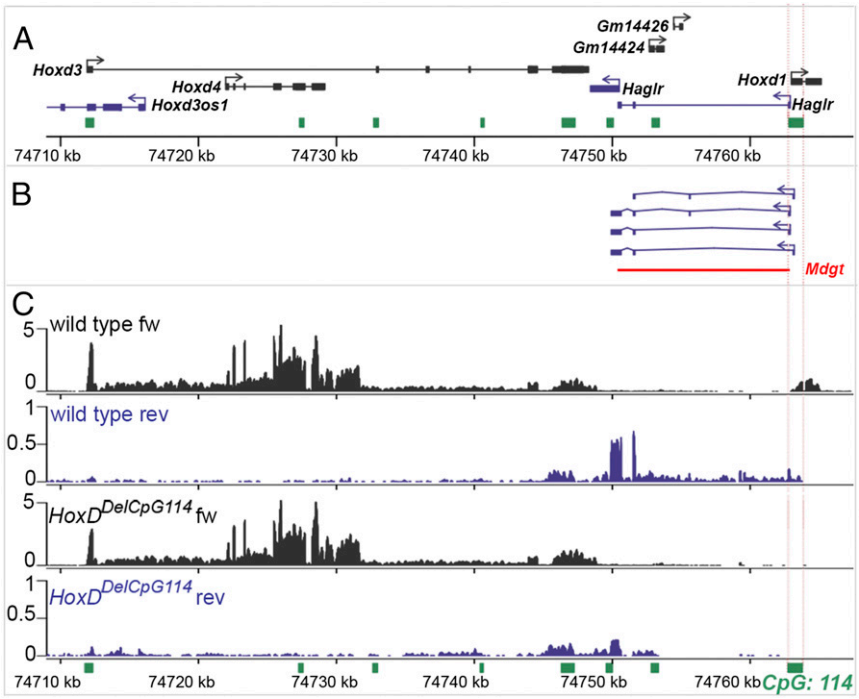

Fig. 6. Targeted deletion and inversion of the CpG114 island that contains the bidirectional *Hoxd1/Haglr* promoter. (*A*) Map of the *Hoxd3-Hoxd1* genomic locus showing annotated transcripts in the Ensembl database and eight CpG islands (green). The CpG114 is shown between two vertical dotted red lines and includes the first exons of both *Hoxd1* and the *Haglr* lncRNA. Nucleotide positions below are on the mm10 genome assembly. (*B*) Splice variants of the *Haglr* transcripts, which were added to the Ensembl transcript annotation list in quantifying FPKM values in RNA-seq analyses. (*C*) BED graphs of uniquely mapped reads to the *Hoxd3–Hoxd1* genomic region on chromosome 2 from E9.5 mouse ribo-depleted RNA samples derived from two wild-type controls and two Del(CpG114)-homozygous embryos. Forward (black) and reverse (purple) strands from two biological replicates are combined.

that were homozygous for the deficiency, and none of them suffered from growth retardation.

Clean stocks for both the deficiency and the inversion were further established, and RNAs were isolated from pairs of homozygous and wild-type control siblings at E9 for RNA-sequencing (RNA-seq). Browser Extensible Data (BED) graphs of mapped reads on both the forward and the reverse strands of the *HoxD* cluster indicated that in wild-type mice *Hoxd1*, *Hoxd3*, and *Hoxd4* were all transcribed as expected from the *Hox* forward strand (Fig. 6*C*). On the reverse strand, reads mapping to the *Haglr* locus were clearly recovered, even though the fragments per kilobase of transcript per million mapped reads (FPKM) value was five- to 10-fold reduced compared with *Hox* genes transcripts. In Del(CpG114)-homozygous animals, *Hoxd1* transcripts were missing, as were the long isoforms of *Haglr* on the opposite strand. Nonetheless, a signal was present over the third and fourth exons of the *Haglr* locus. In terms of FPKM values, this was around one order of magnitude below that the wild-type *Haglr* signal. This observation showed that, besides the two *Haglr* promoters in the CpG island 114, at least one other start site contributed to the expression of the last two exons of *Haglr*. When interrogating the transcriptome genome-wide, only two loci were found with a statistically significant difference after adjusting the *P* values for multiple testing. One was *Hoxd1* and the other *Haglr*, as predicted by the genomic deficiency. Both Del and Inv(CpG114) alleles were bred to homozygosity, but these animals failed to show any slow postnatal weight gain, lethality, or loss of fertility (Table 1). We concluded that neither the deficiency nor the inversion alleles of the CpG1 island 114 had any effect on organismal growth.

Discussion

***HoxD* Cluster-Dependent Gut Maturation and Organismal Growth.** Even though mammalian *Hox* gene functions have been scrutinized in great detail, a potential involvement in postnatal growth has remained undocumented. Here we report that four distinct mutant alleles associated with the *HoxD* cluster induced an early postnatal growth deficit. Growth retardation set in early, and a proportion of animals became fatally wasted. It is therefore likely that an important function for this gene cluster, probably linked to the proper morphogenesis of the gut, was impaired in these various alleles. We followed surviving individuals and determined that growth was systematically resumed once milk feeding was terminated. During this recovery period, the initially reduced excrement size and mass grew, showing an improvement of gut function along with an increase in body mass. Escapers formed small pellets reflecting a retarded expansion of their proximal colon. In addition, the initially meager total dropping mass improved progressively, indicating a delayed expansion of their distal colon.

Likewise, we also noticed that fatally stunted individuals suffered from partial atresia of the proximal colon. In addition, epithelial dysgenesis in the small bowel was noticed in both homozygous $Hoxd3^{hd}$- and $HoxD^{Del(1–9)d10hd}$-mutant specimens, in the latter case with severe enterocyte necrosis at the end of the first week of age. This extensive epithelial cell erosion in $HoxD^{Del(1–9)d10hd}$-homozygous mice is somewhat reminiscent of necrotizing enterocolitis mouse models, which present similar pathological features (17). The repeated occurrence of such pathological deviations in small and large intestine in *HoxD* mutants provides evidence for a broad dysfunction along the intestine at the time the animals fed on milk. Interestingly, previous work involving *Hox* genes reported problems either in producing milk or in the proper regulation of these genes' expression during mammary gland development (18, 19), showing the diverse panel of functions that these genes likely acquired to accompany the emergence of lactation (20).

Notably, this *Hox*-dependent inability to thrive on a milk diet followed by a more-or-less efficient recovery after weaning adds a further piece to the genetic study of milk-adapted gut function.

Previous work has shown that a distinct genetic program was in place in mice to ensure that milk digestion remained active for the necessary period of time. In the absence of *Blimp1*, for example, early enterocytes are lost prematurely, precluding growth of the organism due to the incompetence of the adult-type enterocytes to digest milk (21, 22). Our observations suggest that, similar to *Blimp1*, *Hoxd3* may promote the maintenance of milk-digesting enterocytes, raising the possibility that the two genes belong to the same genetic pathway, even if *Blimp1* function is required in the epithelium whereas *Hoxd3* gene expression is restricted to mesenchymal cells (22–24). The importance of *Hoxd* genes for the patterning of gut mesenchyme derivatives, such as sphincters (25, 26), has been well documented. However, with exception of the ano-rectal transitory epithelium (27), direct function of the *HoxD* cluster in gut epithelium seems unlikely, and hence any functional mechanism linking mesenchymal *Hoxd3* expression to enterocyte survival may imply epithelial–mesenchymal interactions.

Essential Function of *Hoxd3* in Gut Development. Clearly, *Hoxd3* is the major *Hoxd* gene involved in this particular aspect of gut development, as determined by our genetic approaches. Indeed, the loss of function of this gene alone was sufficient to elicit severe growth retardation in homozygous animals. While this phenotype was not described in previously reported studies in which *Hoxd3* was inactivated (6, 7), it was likely observed but not characterized in detail. *Hoxd3* is nevertheless not the only *Hoxd* gene to contribute to proper gut formation, since, although the single loss of function of *Hoxd1*, *Hoxd4*, *Hoxd8*, or *Hoxd9* did not generate any discernable phenotype, combined loss of function *in cis* in addition to *Hoxd3* strengthened the severity of the alterations. For instance, homozygous $HoxD^{Del(1–4)}$ animals in which *Hoxd1*, *Hoxd3*, and *Hoxd4* were all missing displayed a phenotype stronger than that in the simple *Hoxd3*-mutant specimens. However, growth retardation in the latter condition was not as strong as in homozygous $HoxD^{Del(1–9)d10hd}$ animals in which *Hoxd8* and *Hoxd9* had also been removed. It is possible that *Hoxd* genes other than *Hoxd3* can compensate for the lack of function of the latter, even though they may not functionally contribute in the wild-type context. Alternatively, they may have a genuine function that is perhaps too subtle to be revealed in the presence of the HOXD3 protein.

Remarkably, the strongest allele in the series was the $HoxD^{Del(1–9)}$ chromosome, as even heterozygous animals displayed a strong growth deficit. This heterozygous condition was largely rescued when the *Hoxd10* gene was inactivated on the same chromosome, demonstrating that most of the dominant phenotype was induced by a gain of function of this gene, likely following its relocation as the now-leading *Hoxd* gene on the telomeric side of the gene cluster. While such gain of expression of *Hoxd* genes flanking the breakpoints of internal cluster deletions have been documented in the past in a variety of developmental contexts (28–30), the mechanism underlying this dominant-negative effect remains to be fully clarified. The HOXD10 protein ectopically expressed with the *Hoxd3* tissue specificity may trigger an inappropriate genetic program leading to the misspecification of gut morphology.

Nevertheless, we favor an alternative explanation whereby HOXD10 exerts its dominant-negative effect upon other, more anterior *Hox* genes such as *Hoxd3*. This dominant-negative effect of some posterior HOX proteins over more anterior members of the same family ["posterior prevalence" (31–33)] has been documented in a variety of situations (8, 30, 34, 35). In this view, the gain of *Hoxd10* expression following its new genomic position within the gene cluster would affect the function of all anterior HOX proteins, somewhat equivalent to a global homozygous loss of function of *Hox* genes. The fact that many heterozygous $HoxD^{Del(1–9)}$ animals were as strongly affected as homozygous $HoxD^{Del(1–9)10hd}$ animals and displayed a very related phenotype involving gut morphology supports this explanation. As a consequence, the $HoxD^{Del(1–9)}$-heterozygous condition would be merely yet another loss-of-function *HoxD* allele, one produced by the dominant-negative interference of the HOXD10 protein. Since rescuing the mutation of *Hoxd10* in the $HoxD^{Del(1–9)}$ chromosome involves a microdeletion into its DNA-binding domain, it is possible that this dominant effect requires the binding of HOXD10 to DNA target sites normally occupied by other HOX proteins. In this particular case, we consider other proposed mechanisms to trigger this negative effect, such as disturbed interactions with cofactors of the TALE homeodomain protein family (36, 37) or the involvement of microRNAs (35), as less plausible.

Is the LncRNA *Haglr* Involved in Postnatal Growth? According to the description of *Mdgt* mice, i.e., animals lacking the lncRNA *Haglr* (3), $HoxD^{Del(1–9)}$-heterozygous animals and $Hoxd3^{hd}$-homozygous specimens suffered from a comparable slow postnatal weight gain. In the $HoxD^{Del(1–9)}$ animals, however, a full wild-type haplotype of the *HoxD* cluster was present, including an intact copy of *Haglr*, whereas in $Hoxd3^{hd}$ mice both *Haglr* loci were intact. The $Hoxd3^{hd}$ phenotype was particularly intriguing, since the *Haglr* RNA extends up to the 3′ end of the *Hoxd3* UTR, thus raising the possibility that the deletion of *Haglr* would, in fact, affect the function of *Hoxd3* (11). To verify this hypothesis, a transcriptome analysis of *Midget* mice would be necessary. On our side, we investigated this alternative by trying to knock down *Haglr* transcription while preserving the activity of *Hoxd3*. The targeted deletion of CpG114 indeed abrogated all long isoforms of the *Haglr* transcript in E9.5 embryos, corresponding to the extent of the deletion reported in ref. 3. In these embryos, the *Hoxd3* transcripts were normal in all respects. Despite the absence of *Haglr* transcripts, growth deficit was not observed in homozygous mice, indicating that variation of *Haglr* RNA level had no appreciable consequence in organismal growth.

Shorter transcripts were nevertheless still initiated from the anti-*Hox* strand in the Del(CpG114) chromosome (although at a much lower level) and terminated exactly at the position of the termination site of the *Hoxd3* UTR (Fig. 6). These transcripts, which were also named "*Haglr*" in the Ensembl database even though they have an independent start site, initiated within the last exon of *Haglr*. It is not known whether such transcripts are still present in *Midget* mice after the large targeted deletion and *lacZ* reporter replacement (3). If these additional RNAs were not maintained in *Mdgt* embryos, it is possible that their absence would perturb the transcription of *Hoxd3*, thus leading to growth retardation. In such a scenario, however, the function of these RNAs would be exerted *in cis* rather than *in trans* (38), as a result of transcriptional interference. Taking these results together, we conclude that the effect of the *Mdgt* deletion is more likely due to the extent of the genomic deficiency or the insertion of foreign DNA such as the *LacZ* transcription unit over the *Hoxd3* gene rather than to the absence of the specific *Haglr* transcript. This lncRNA may result from a bidirectional transcription at the *Hoxd1* start site (39) and may not have any particular function in controlling postnatal growth.

Materials and Methods

Mouse Strains. Mice were handled according to the Swiss law on animal protection (LPA) with the authorizations GE/81/14 (to D.D.) and GE/29/26 (to B.M.). Animal experiments were agreed upon by the ethical committee of the Canton of Geneva. Genetically modified mice were maintained and crossed in heterozygosis. All CRISPR/Cas9 alleles were produced by pronuclear injection (40) of the pX330:hSpCas9 (Addgene ID 42230) vector with the appropriate guide-sequence oligos cloned as recommended (41). When deletions or inversions between two guide sequences were intended, the appropriate plasmids were injected in equimolar solution.

Zygotes were derived from (B6CBA)F1 females crossed to (B6CBA)F1 males. Founder animals were crossed with males or females of the (B6CBA)F1 wild-type genotype, and routine strain maintenance was continued by crossing heterozygous males of the allele in question to (B6CBA)F1 wild-type females.

Target sequences were identified using the web tool at crispr.mit.edu during the year 2013. Nucleotide positions are based on GRCm38/mm10.

The production of the various mutant alleles used in this study is described in the *SI Materials and Methods* section.

RNA Extraction and RNA-Seq. RNA extraction and RNA-seq were as described in ref. 18. *Haglr* transcript isoforms were cloned and sequenced starting from an E8 mouse tail-bud total RNA preparation as a source for first-strand cDNA synthesis using SuperScript II reverse transcriptase from Invitrogen, following the manufacturer's protocol. cDNA was amplified using Phusion High Fidelity DNA polymerase from Thermo Scientific. Amplicons were cloned into the pGEM-T Easy plasmid vector (A1360; Promega) and transformed into JM109 cells; cloned and plasmid DNA samples were isolated by the Qiagen Midi protocol. RNA-seq–processed and raw datasets were deposited in the Gene Expression Omnibus (GEO) database with accession number GSE103086.

Histology and Coprometric Analyses. For histology and coprometric analyses, see *SI Materials and Methods*.

ACKNOWLEDGMENTS. We thank members of the D.D. laboratories for sharing material and discussions, the histology platform at Ecole Polytechnique Fédérale (Lausanne) (EPFL), the genomics platform in Geneva, Olivier Schaad for advice on statistical analyses, and Thomas Alexander McKee for discussions. This work was supported by funds from the EPFL, the University of Geneva, Swiss National Research Fund Grant 310030B_138662, European Research Council Grants System*Hox* 232790 and Regul*Hox* 588029, and the Claraz Foundation (D.D.).

1. Spitz F, et al. (2001) Large scale transgenic and cluster deletion analysis of the HoxD complex separate an ancestral regulatory module from evolutionary innovations. *Genes Dev* 15:2209–2214.
2. Zakany J, Duboule D (2012) A genetic basis for altered sexual behavior in mutant female mice. *Curr Biol* 22:1676–1680.
3. Sauvageau M, et al. (2013) Multiple knockout mouse models reveal lincRNAs are required for life and brain development. *Elife* 2:e01749.
4. Guo T, et al. (2011) An evolving NGF-Hoxd1 signaling pathway mediates development of divergent neural circuits in vertebrates. *Nat Neurosci* 14:31–36.
5. Zákány J, Kmita M, Alarcon P, de la Pompa JL, Duboule D (2001) Localized and transient transcription of Hox genes suggests a link between patterning and the segmentation clock. *Cell* 106:207–217.
6. Condie BG, Capecchi MR (1993) Mice homozygous for a targeted disruption of Hoxd-3 (Hox-4.1) exhibit anterior transformations of the first and second cervical vertebrae, the atlas and the axis. *Development* 119:579–595.
7. Greer JM, Puetz J, Thomas KR, Capecchi MR (2000) Maintenance of functional equivalence during paralogous Hox gene evolution. *Nature* 403:661–665.
8. Zacchetti G, Duboule D, Zakany J (2007) Hox gene function in vertebrate gut morphogenesis: The case of the caecum. *Development* 134:3967–3973.
9. Delpretti S, et al. (2013) Multiple enhancers regulate Hoxd genes and the Hotdog LncRNA during cecum budding. *Cell Rep* 5:137–150.
10. Tschopp P, Christen AJ, Duboule D (2012) Bimodal control of Hoxd gene transcription in the spinal cord defines two regulatory subclusters. *Development* 139:929–939.
11. Bassett AR, et al. (2014) Considerations when investigating lncRNA function in vivo. *Elife* 3:e03058.
12. Tschopp P, Duboule D (2011) A genetic approach to the transcriptional regulation of Hox gene clusters. *Annu Rev Genet* 45:145–166.
13. Tarchini B, Duboule D (2006) Control of Hoxd genes' collinearity during early limb development. *Dev Cell* 10:93–103.
14. Duboule D, Morata G (1994) Colinearity and functional hierarchy among genes of the homeotic complexes. *Trends Genet* 10:358–364.
15. Horan GS, Kovàcs EN, Behringer RR, Featherstone MS (1995) Mutations in paralogous Hox genes result in overlapping homeotic transformations of the axial skeleton: Evidence for unique and redundant function. *Dev Biol* 169:359–372.
16. Gouat P (1992) Faecal pellet size difference as a field criterion to distinguish between two Ctenodactylus species (Mammalia, Rodentia). *Z Saugetierkd* 57:183–185.
17. Neal MD, et al. (2013) A critical role for TLR4 induction of autophagy in the regulation of enterocyte migration and the pathogenesis of necrotizing enterocolitis. *J Immunol* 190:3541–3551.
18. Chen F, Capecchi MR (1999) Paralogous mouse Hox genes, Hoxa9, Hoxb9, and Hoxd9, function together to control development of the mammary gland in response to pregnancy. *Proc Natl Acad Sci USA* 96:541–546.
19. Schep R, et al. (2016) Control of Hoxd gene transcription in the mammary bud by hijacking a preexisting regulatory landscape. *Proc Natl Acad Sci USA* 113:E7720–E7729.
20. Duboule D (1999) No milk today (my Hox have gone away). *Proc Natl Acad Sci USA* 96:322–323.
21. Harper J, Mould A, Andrews RM, Bikoff EK, Robertson EJ (2011) The transcriptional repressor Blimp1/Prdm1 regulates postnatal reprogramming of intestinal enterocytes. *Proc Natl Acad Sci USA* 108:10585–10590.
22. Muncan V, et al. (2011) Blimp1 regulates the transition of neonatal to adult intestinal epithelium. *Nat Commun* 2:452.
23. Gurdziel K, Vogt KR, Walton KD, Schneider GK, Gumucio DL (2016) Transcriptome of the inner circular smooth muscle of the developing mouse intestine: Evidence for regulation of visceral smooth muscle genes by the hedgehog target gene, cJun. *Dev Dyn* 245:614–626.
24. Tan DP, Shao X, Pu L, Guo V, Nirenberg M (1996) Sequence and expression of the murine Hoxd-3 homeobox gene. *Proc Natl Acad Sci USA* 93:8247–8252.
25. Kondo T, Dollé P, Zákány J, Duboule D (1996) Function of posterior HoxD genes in the morphogenesis of the anal sphincter. *Development* 122:2651–2659.
26. Zákány J, Duboule D (1999) Hox genes and the making of sphincters. *Nature* 401:761–762.
27. Dollé P, Izpisúa-Belmonte JC, Boncinelli E, Duboule D (1991) The Hox-4.8 gene is localized at the 5′ extremity of the Hox-4 complex and is expressed in the most posterior parts of the body during development. *Mech Dev* 36:3–13.
28. Kmita M, Tarchini B, Duboule D, Hérault Y (2002) Evolutionary conserved sequences are required for the insulation of the vertebrate Hoxd complex in neural cells. *Development* 129:5521–5528.
29. Zákány J, Kmita M, Duboule D (2004) A dual role for Hox genes in limb anterior-posterior asymmetry. *Science* 304:1669–1672.
30. Kmita M, van Der Hoeven F, Zákány J, Krumlauf R, Duboule D (2000) Mechanisms of Hox gene colinearity: Transposition of the anterior Hoxb1 gene into the posterior HoxD complex. *Genes Dev* 14:198–211.
31. Struhl G (1983) Role of the esc+ gene product in ensuring the selective expression of segment-specific homeotic genes in Drosophila. *J Embryol Exp Morphol* 76:297–331.
32. González-Reyes A, Urquia N, Gehring WJ, Struhl G, Morata G (1990) Are cross-regulatory interactions between homoeotic genes functionally significant? *Nature* 344:78–80.
33. Bachiller D, Macías A, Duboule D, Morata G (1994) Conservation of a functional hierarchy between mammalian and insect Hox/HOM genes. *EMBO J* 13:1930–1941.
34. van der Hoeven F, Zákány J, Duboule D (1996) Gene transpositions in the HoxD complex reveal a hierarchy of regulatory controls. *Cell* 85:1025–1035.
35. Yekta S, Tabin CJ, Bartel DP (2008) MicroRNAs in the Hox network: An apparent link to posterior prevalence. *Nat Rev Genet* 9:789–796.
36. Rivas ML, et al. (2013) Antagonism versus cooperativity with TALE cofactors at the base of the functional diversification of Hox protein function. *PLoS Genet* 9:e1003252.
37. Bürglin TR, Affolter M (2016) Homeodomain proteins: An update. *Chromosoma* 125:497–521.
38. Gummalla M, et al. (2012) abd-A regulation by the iab-8 noncoding RNA. *PLoS Genet* 8:e1002720.
39. Sigova AA, et al. (2013) Divergent transcription of long noncoding RNA/mRNA gene pairs in embryonic stem cells. *Proc Natl Acad Sci USA* 110:2876–2881.
40. Mashiko D, et al. (2013) Generation of mutant mice by pronuclear injection of circular plasmid expressing Cas9 and single guided RNA. *Sci Rep* 3:3355.
41. Cong L, et al. (2013) Multiplex genome engineering using CRISPR/Cas systems. *Science* 339:819–823.
42. Padmanabhan P, Grosse J, Asad AB, Radda GK, Golay X (2013) Gastrointestinal transit measurements in mice with 99mTc-DTPA-labeled activated charcoal using Nano-SPECT-CT. *EJNMMI Res* 3:60.
43. Hérault Y, Rassoulzadegan M, Cuzin F, Duboule D (1998) Engineering chromosomes in mice through targeted meiotic recombination (TAMERE). *Nat Genet* 20:381–384.
44. Theiler K (1989) *The House Mouse. Atlas of Embryonic Development* (Springer, New York), p 150.
45. Walthall K, Cappon GD, Hurtt ME, Zoetis T (2005) Postnatal development of the gastrointestinal system: A species comparison. *Birth Defects Res B Dev Reprod Toxicol* 74:132–156.